Characterization of the DNA-Binding Domains from the Yeast Cell-Cycle Transcription Factors Mbp1 and Swi4

Ian A. Taylor,[‡] Pauline B. McIntosh,[§] Preshna Pala,[‡] Monika K. Treiber,[‡] Steven Howell,[‡] Andrew N. Lane,[§] and Stephen J. Smerdon*,[‡]

Divisions of Protein Structure and Molecular Structure, National Institute for Medical Research, The Ridgeway, Mill Hill, London NW7 1AA, United Kingdom

Received September 23, 1999; Revised Manuscript Received December 27, 1999

ABSTRACT: The minimal DNA-binding domains of the *Saccharomyces cerevisiae* transcription factors Mbp1 and Swi4 have been identified and their DNA binding properties have been investigated by a combination of methods. An ∼100 residue region of sequence homology at the N-termini of Mbp1 and Swi4 is necessary but not sufficient for full DNA binding activity. Unexpectedly, nonconserved residues C-terminal to the core domain are essential for DNA binding. Proteolysis of Mbp1 and Swi4 DNA−protein complexes has revealed the extent of these sequences, and C-terminally extended molecules with substantially enhanced DNA binding activity compared to the core domains alone have been produced. The extended Mbp1 and Swi4 proteins bind to their cognate sites with similar affinity [$K_A \sim (1-4) \times 10^6$ M^{-1}] and with a 1:1 stoichiometry. However, alanine substitution of two lysine residues (116 and 122) within the C-terminal extension (tail) of Mbp1 considerably reduces the apparent affinity for an MCB (*Mlu*I cell-cycle box) containing oligonucleotide. Both Mbp1 and Swi4 are specific for their cognate sites with respect to nonspecific DNA but exhibit similar affinities for the SCB (Swi4/Swi6 cell-cycle box) and MCB consensus elements. Circular dichroism and ^{1}H NMR spectroscopy reveal that complex formation results in substantial perturbations of base stacking interactions upon DNA binding. These are localized to a central 5′-d(C-A/G-CG)-3′ region common to both MCB and SCB sequences consistent with the observed pattern of specificity. Changes in the backbone amide proton and nitrogen chemical shifts upon DNA binding have enabled us to experimentally define a DNA-binding surface on the core N-terminal domain of Mbp1 that is associated with a putative winged helix−turn−helix motif. Furthermore, significant chemical shift differences occur within the C-terminal tail of Mbp1, supporting the notion of two structurally distinct DNA-binding regions within these proteins.

Transcription in eukaryotes is a complex process that must be tightly controlled. This regulation is often achieved through interactions between combinatorial arrays of transcription factors that respond to variations in chromatin structure and chemical modification. Transcriptional complexes may be found on specific DNA sequences within the promoter or at distal sites that are often located at a considerable distance from it (for reviews see refs *1* and *2*). Proteins that make up many of the complexes involved in these processes are often modular, multidomain molecules. These domains may be variously required for detection of extranuclear signals, targeted enzymatic activity, sequence-specific DNA binding, or mediation of interactions with other coregulatory proteins. Interplay between these protein complexes is essential for the execution of a successful and correctly timed transcriptional initiation program.

MBF[1] (*Mlu*I cell-cycle box binding factor) and SBF (Swi4/Swi6 cell-cycle box binding factor) are two large protein complexes involved in transcriptional regulation in the budding yeast *Saccharomyces cerevisiae*. These proteins bind to short DNA sequences distal to target promoters and regulate the transcription of many genes during the G1−S transition of the cell cycle. MBF and SBF each contain the Swi6 protein (*3*) and one of two distinct DNA binding proteins, Swi4 in SBF (*4*, *5*) or Mbp1 in MBF (*6*). SBF complexes bind to sequences known as SCBs (Swi4/Swi6-dependent cell-cycle box). These are often present in multiple copies and have the consensus sequence 5′-d(CACGAAA) (*7*). Similarly, genes encoding proteins required for DNA replication are regulated by binding of MBF to sequences called MCBs (*Mlu*-I cell-cycle box) that have the similar consensus sequence 5′-d(ACGCGTNA) (*8*). In the fission yeast *Schizosaccharomyces pombe*, similar complexes of the Cdc10 protein with Res1/Sct1 or Res2/Pct1 bind to MCB sequences and regulate transcription at Start or direct movement into premeiotic S-phase (*9*).

Swi6, Swi4, and Mbp1 together with Cdc10, Res1, and Res2 form a closely related family of transcription factors that share several regions of sequence homology. Structural

* To whom correspondence should be addressed: Telephone ++44 181 959 3666, ext 2533; FAX ++44 181913 8569; E-mail s-smerdo@darwin.nimr.mrc.ac.uk.

[‡] Division of Protein Structure.

[§] Division of Molecular Structure.

[1] Abbreviations: MCB, *Mlu*I cell-cycle box; SCB, Swi4/Swi6 cell-cycle box; MBF, *Mlu*I cell cycle box binding factor; SBF, Swi4/Swi6 cell cycle box binding factor; wHTH, winged helix−turn−helix; HNF3γ, hepatocyte nuclear factor 3γ; CD circular dichroism.

10.1021/bi992212i CCC: $19.00
Published on Web 03/11/2000

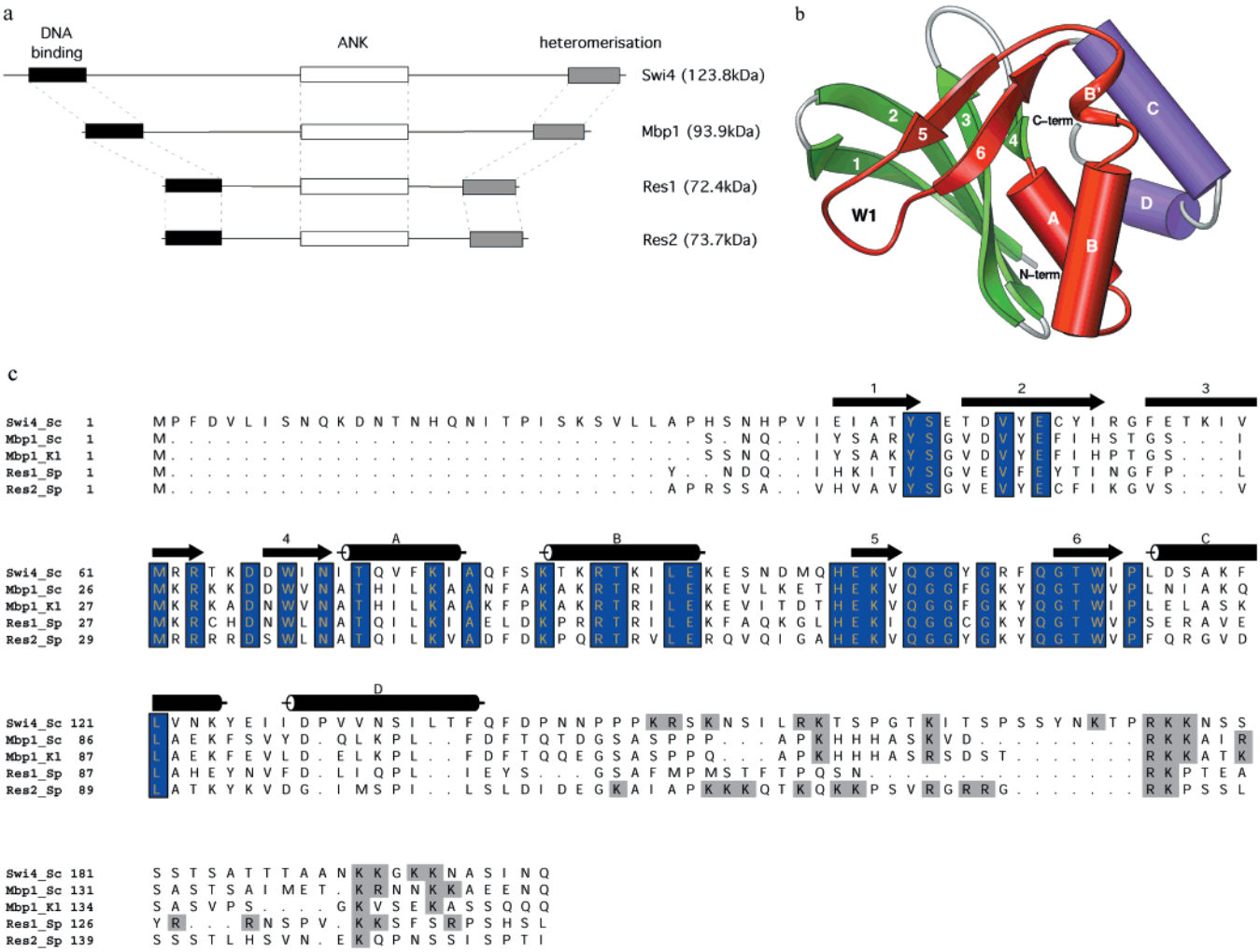

FIGURE 1: (a) Schematic representation of the extent and distribution of the major regions of sequence homology between Swi4, Mbp1, Res1, and Res2 (ANK = ankyrin repeats). (b) Structure of Mbp1(124) determined by X-ray crystallography (*21*; PDB accession code 1MB1) shown as a ribbon representation with helices depicted as cylinders. The secondary structural elements are labeled as described previously. The helix−turn−helix motif (αA and B and associated *β*-loop, strands 5 and 6; w1) are colored red. (c) Sequence alignment of the N-terminal regions from *Saccharomyces cerevisiae* (Sc) Mbp1, Swi4 with related proteins from *Schizosaccharomyces pombe* (Sp) and *Kluyveromyces lactis* (Kl). Regions of sequence identity are highlighted in blue and the secondary structural elements are highlighted. The alignment extends into the C-terminal region, where sequence conservation is undetectable. The alignment in this region has been manually edited largely to overlap basic residues that are highlighted in gray.

domains in Swi6 have been defined in vitro by limited proteolytic mapping and functionality ascribed to individual domains in vivo by the use of deletion analysis coupled with transcriptional activation assays (*10*). With this information and sequence homology, three functional regions within these molecules can be defined (Figure 1a). Conserved sequences at the C-termini encompass a putative helical domain that has been shown to mediate protein−protein interactions required for the formation of heteromeric complexes (*11*, *12*). A central domain contains five copies of the ankyrin repeat motif, originally predicted from sequence comparisons (*13*, *14*) and now confirmed by X-ray crystallographic studies of Swi6 (*15*). The ankyrin repeats and associated structures appear to be involved in interactions with B-type cyclins, cyclin−CDK complexes, and other coregulatory molecules (*12*, *16*−*18*).

The DNA-binding activities of SBF and MBF reside within the N-terminal regions of Swi4 and Mbp1 (*6*, *19*). The X-ray structure of an N-terminal 124 residue fragment of Mbp1 (*20*, *21*) (Figure 1b) has revealed a topological relationship to the winged helix−turn−helix (wHTH) family of DNA-binding proteins. Alignment of the structure of the Mbp1 DNA binding domain with that of the archetypal wHTH protein HNF3*γ* (*22*) strongly suggests that helix B is the major sequence recognition element through base-specific interactions in the major groove. The N-terminal regions of Swi4 and Mbp1 are highly homologous to those of Res1 and Res2 from *S. pombe* (Figure 1c). Homologous segments have also been identified in several other transcriptional regulators indicating that this motif may be commonly used in other species. It is therefore likely that the same fold will be present in all of these molecules and that they all utilize a common mode of DNA recognition.

The sequence and structural similarities between these transcription factors provide an opportunity to examine the molecular basis of nucleic acid interaction and sequence recognition in a closely related group of DNA-binding proteins. Although structural information and some biochemical data are available, the affinities of the DNA−protein interactions, the extent of the minimal DNA-binding domain, and the exact nature of the cross-competition between MCB and SCB elements remain unclear. Here we

report a series of biochemical and spectroscopic studies that directly address these questions. Our data indicate that Mbp1, Swi4, and related transcription factors appear to utilize an unusual mode of DNA binding. A highly conserved domain provides sequence specificity while nonconserved sequences located C-terminal to this region appear to contribute to the overall DNA affinity, most likely through structural effects on the core domain and/or nonspecific electrostatic interactions with the DNA.

EXPERIMENTAL PROCEDURES

Protein Expression and Purification. The coding regions corresponding to N-terminal fragments derived from Mbp1 and Swi4 were produced by PCR amplification from plasmid templates containing the full-length Mbp1 and Swi4 genes. Fragments were expressed in the *Escherichia coli* strain BL21(DE3) as C-terminal hexahistidine fusions from the T7 expression vector pET22b (Novagen). The various proteins were purified from clarified crude cell extracts by ion-exchange, immobilized metal-ion affinity, and gel-filtration chromatography.

The purity and monodispersity of preparations were analyzed by SDS−PAGE, photon correlation spectroscopy, and analytical size-exclusion chromatography. Protein concentrations were determined from the absorbance at 280 nm with molar extinction coefficients derived by summing the contributions from tyrosine and tryptophan residues: Mbp1-(110), Mbp1(124), Mbp1(151), and Swi4(165), 17 900 M^{-1} cm^{-1}, and Swi4(202) and Swi4(32−173), 19 200 M^{-1} cm^{-1}.

Preparation of Oligonucleotide Duplexes. In total, three synthetic DNA duplexes, MCB1, SCB1, and MCB12T, were used in DNA binding experiments. Duplexes were prepared from HPLC-purified oligonucleotides (Oswel DNA services, University of Southampton, U.K.):

MCB1

5′-CCGCTGCAGGTG**ACGCGTAA**GCTTGGC-3′

3′-GGCGACGTCCAC**TGCGCATT**CGAACCG-5′

SCB1

5′-CCGAAGCTTGAAGTA**CACGAAA**TTCGGATATCGGC-3′

3′-GGCTTCGAACTTCAT**GTGCTTT**AAGCCTATAGCCG-5′

MCB12T

5′-TTTG**ACGCGTCA**A-3′

3′-A**ACTGCGCA**GTTT-5′

To ensure accurate mixing of single strands in equimolar proportions, molar extinction coefficients were determined for each oligonucleotide. This was done by summing the contribution from the individual nucleotides, taking into account the hyperchromicity observed following digestion by snake venom phosphodiesterase I (*23*). Duplexes were then prepared by mixing complementary strands in equimolar proportions, except the self-complementary MCB12T. In all cases annealing reactions were then heated to 95 °C for 5 min and cooled slowly to 4 °C over 4 h. Duplex DNAs were purified by gel-filtration chromatography on Superose-12 HR (12/30) (Pharmacia) and molar extinction coefficients were determined as for the single strands. The values derived for the three duplexes (M^{-1} cm^{-1}) were $\epsilon_{260,MCB1} = 374\,000$, $\epsilon_{260,SCB1} = 478\,100$, and $\epsilon_{260,MCB12T} = 193\,300$.

Gel-Retardation Assays. Typically ∼1 nmol of a duplex was end-labeled with [γ-^{32}P]ATP and T4 polynucleotide kinase with standard protocols. The labeled DNA was purified from unincorporated ATP on a NICK spin column (Pharmacia) and then ethanol-precipitated. Labeled DNA was resuspended in a solution of unlabeled duplex such that the concentration was between 100 and 200 μM. The concentration was then determined accurately from the absorbance at 260 nm. DNA binding reactions for both titration and competition experiments were carried out in a binding buffer containing 10% glycerol, 5 mM $MgCl_2$, 1 mM DTT, and 40 mM Tris-HCl pH 8.0. In titration experiments, increasing amounts of protein were incubated with a fixed concentration of either MCB1 or SCB1 labeled DNA. In competition experiments Mbp1(124) or Swi4(32−173) was added to an equimolar amount of either labeled MCB1 or SCB1 in the presence of increasing amounts of unlabeled competitor DNA. The free and bound components of the equilibria were resolved by electrophoresis at 14 mA constant current for 45 min on 8% native TAE gels (40 mM Tris−acetate and 1 mM EDTA, pH 8.5). The labeled components were visualized either by autoradiography or by phosphorimaging.

Limited Proteolysis. In proteolysis experiments, Mbp1-(151) and Swi4(202) were buffer-exchanged into digestion buffer (20 mM Tris-HCl, 100 mM NaCl, 1 mM EDTA, and 3 mM DTT, pH 7.8) using NAP5 columns (Pharmacia). Proteolytic digestion with trypsin (Boehringer Mannheim, sequencing grade) was carried out at an enzyme-to-protein ratio of either 1:250 or 1:500 (w/w) and at a protein concentration between 0.6 and 1.2 mg/mL. Where appropriate, either MCB1 or SCB1 was added at a 1.2-fold molar excess. Products of time courses of digestion were separated by electrophoresis on SDS−18% polyacrylamide gels and visualized by staining with Coomassie brilliant blue. To analyze the proteolytic products by mass spectrometry, digestion products were purified either by ion exchange on Mono S or by reverse-phase chromatography on Zorbax 300SB-C3. Peptide molecular weights were determined with a modified 130A HPLC (Perkin-Elmer) coupled on-line to a Platform electrospray mass spectrometer (Micromass, U.K.). Reverse-phase chromatography of purified peptides was performed on a 0.25 mm × 100 mm PEEK column packed in-house with Poros RII (PerSeptive Biosystems) medium. Peptides were eluted at a flow rate of 10 μL/min over a 10 min, 0−100% buffer B linear gradient (buffer A = 0.12% formic acid, 90% water, and 10% acetonitrile; buffer B = 0.10% formic acid, 15% water, and 85% acetonitrile) with UV monitoring at $\lambda = 214$ nm. The low flow rate was achieved by incorporating a Valco tee, coupled to a microbore dummy column, just prior to the Rheodyne injection valve. The mass spectrometer was calibrated with myoglobin as a standard.

Site-Directed Mutagenesis. The Mbp1(124)-pET22b expression plasmid was used as a template for mutagenesis of Mbp1(124). Three Lys → Ala substitutions (K116A, K122A, and K116A/K122A) were generated with a QuikChange site-directed mutagenesis kit (Stratagene), following the manufacturer's instructions. Base changes were identified by DNA sequencing and later confirmed by ESI-MS analysis of the purified mutant proteins.

Circular Dichroism Spectroscopy. Circular dichroism (CD) spectroscopy was used to analyze the binding of Mbp1(124) to the MCB12T duplex. Near UV CD spectra (330−230 nm)

were recorded in 1 cm cells at 15 °C in 40 mM NaH_2PO_4/Na_2HPO_4 and 100 mM NaCl, pH 7.6, using a Jasco J600 spectropolarimeter purged with nitrogen gas. Titrations were carried out with a fixed concentration of MCB12T (4.68 μM) and varying protein concentrations from 0 to 14.4 μM. The contribution of the protein and buffer background to each spectrum was subtracted. Subsequent inspection of spectra revealed a large signal change at around 270 nm that was used to construct binding curves. The protein contribution to the overall signal at 270 nm amounts to ~15% at a molar excess (protein:DNA) of 3:1.

NMR Spectroscopy. Protein and DNA samples were prepared for NMR spectroscopy as previously described (*24*). ^{1}H and ^{1}H−^{15}N NMR spectra were recorded at 11.75 or 14.1 T on Varian UnityPlus or Unity spectrometers, respectively. ^{31}P NMR spectra were recorded at 9.4 T on a Bruker AM400 spectrometer. All spectra were recorded at 15 °C.

Quantitation of Binding Data. Data from titration experiments were analyzed with a general binding expression, eq 1. This expression relates the association constant K_a to the fraction of bound DNA sites θ (θ = [PD]/[Dt], where [PD] is the concentration of protein−DNA complex) in terms of the total concentrations of DNA binding sites [Dt] and protein [Pt] (*25*). For CD titrations, rearrangement of eq 1 to give eq 2 allows K_a and [Dt] to be determined by nonlinear fitting of a plot of θ versus [Dt].

$$K_a = \theta/(1 - \theta)([Pt] - \theta[Dt]) \quad (1)$$

$$\theta = [(K_a[Pt] + K_a[Dt] + 1) - \{(K_a[Pt] + K_a[Dt] + 1)^2 - (4K_a^2[Dt][Pt])\}^{1/2}]/2K_a[Dt] \quad (2)$$

In quantitative gel retardation titration experiments, free and bound band intensities were measured by phosphorimaging (Molecular Dynamics). For these data, binding constants were derived directly from the simplification of eq 1 at the stoichiometric point (i.e. [Pt] = [Dt]):

$$K_a = \theta/[Dt](1 - \theta)^2 \quad (3)$$

In competition experiments, association constants for competitor sites (K_{comp}) were derived by direct nonlinear fitting of experimental data to an expression relating the total concentration of competitor sites ([Ct]) to the fraction of specific sites bound (θ) in terms of the total concentrations of protein and specific DNA sites ([Pt] and [Dt]), and the binding constant for specific sites (K_a):

$$[Ct] = ([Pt] - \theta[Dt])(1 + \{1/K_a[Dt](1 - \theta)\}) \times (1 + K_a[Dt](1 - \theta)/K_{comp}\theta[Dt]) \quad (4)$$

RESULTS

Determination of the Minimal DNA-Binding Domains of Mbp1 and Swi4. To analyze the DNA binding properties of N-terminal fragments from Mbp1 and Swi4, quantitative gel retardation assays were employed together with proteolytic protection analysis. Initially four N-terminal fragments were overexpressed and purified from *Escherichia coli*. Two comprise only the core homology region [residues 1−110 from Mbp1, Mbp1(110), and residues 1−165 from Swi4, Swi4(165)] and two include additional C-terminal sequences (residues 1−151 from Mbp1; Mbp1(151), and 1−202 from Swi4, Swi4(202)]. The sequence of these constructs, along with an alignment of the homologous regions, is shown in Figure 1c. Two oligonucleotide duplexes, MCB1 and SCB1, were prepared for use in the various DNA-binding experiments. MCB1 is a 27 bp fragment containing a single MCB element derived from the *S. cerevisiae* TMP1 promoter, and SCB1 is a 35 bp fragment containing a single SCB element derived from the CLN2 promoter.

The gel retardation titration experiments performed using these Mbp1- and Swi4-derived fragments are shown in Figure 2. All of the titration experiments were carried out under similar conditions (~10 μM duplex). They clearly demonstrate considerable differences in the DNA-binding properties of proteins containing only the core homology region compared with those containing extra C-terminal sequences. The ability to bind stoichiometrically to either the MCB or SCB recognition sequence, as judged by the ratio of free to bound duplex at a 1:1 molar ratio of protein:DNA, is only apparent for the Mbp1(151) and Swi4(202) proteins. Under very similar conditions, Mbp1(110) and Swi4(165) do not form a distinct retarded complex and there remains a large fraction of unbound DNA at the stoichiometric point of the titration. Deletion of the hexahistidine tag or replacing it at the N-terminus has no effect on the DNA-binding activity of any fragment that we have examined (data not shown). All four proteins show similar behavior in dynamic light scattering and analytical gel-filtration experiments, and all have the correct molecular mass as determined by electrospray ionization mass spectrometry (ESI-MS). Thus, aggregation, chemical modification, and denaturation are not responsible for the differential binding properties and the observed enhancement of DNA binding activity can be confidently attributed to the presence of the additional C-terminal sequences.

Limited proteolytic digestion has often proved an invaluable tool for the analysis of DNA−protein interactions (*26*, *27*). In this study, we compared the susceptibility to tryptic digestion of both free Mbp1(151) and Swi4(202) with their respective MCB1 and SCB1 DNA complexes. The time dependence of these tryptic digestions, analyzed by SDS−PAGE, are shown in Figure 3. In the absence of DNA Mbp1-(151) is rapidly cleaved to a stable core fragment that is then slowly degraded to smaller peptides. Digestion of the protein−DNA complex under the same conditions reveals a similar digestion pattern with the exception that the initially produced core fragment is not further degraded during the remainder of the digestion time course. This implies that the DNA protects the core protein fragment. Swi4(202) and its complex with the SCB1 duplex exhibit similar patterns of digestion to those observed for Mbp1(151). Isolated Swi4-(202) is rapidly cleaved to generate a stable fragment that is subsequently slowly degraded. However, in this case species of intermediate molecular mass between that of the full-length protein and the core fragment are generated (T* in Figure 3b). These fragments are not as stable as the final core fragment but they persist only in the presence of DNA and only at later time points.

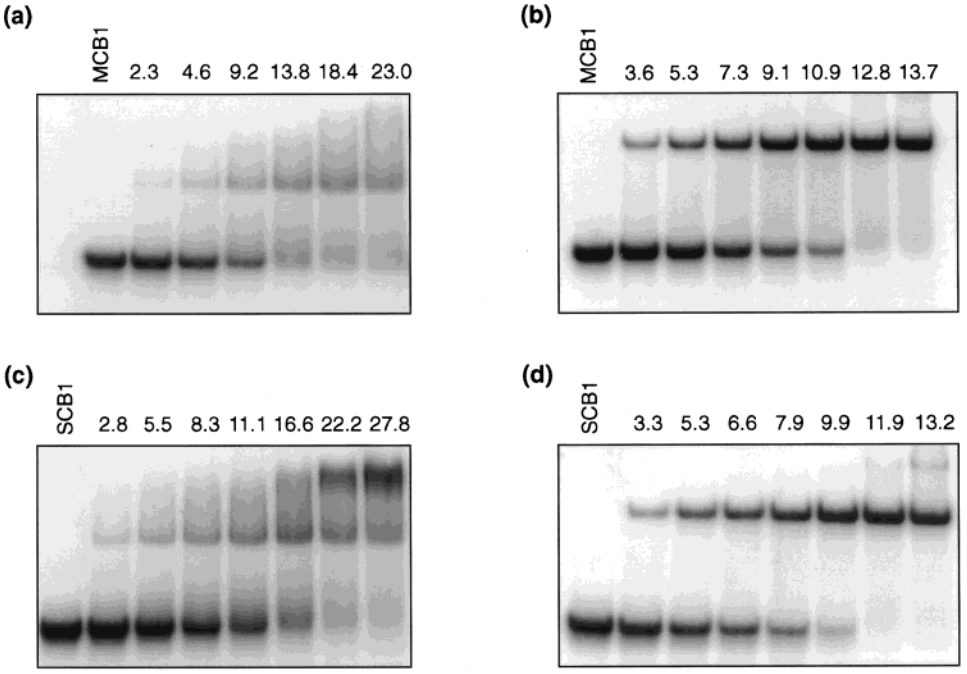

FIGURE 2: Gel-retardation titration assays of core homology and extended DNA binding domains from Mbp1 and Swi4. Panels a and b show titrations of Mbp1(110) and Mbp1(151) with MCB1 at 10.9 and 11.8 μM. Panels c and d show titrations of Swi4(165) and Swi4(202) with SCB1 at 10.3 and 10.5 μM. The protein concentration (micromolar) at each point in the titration is indicated above each track.

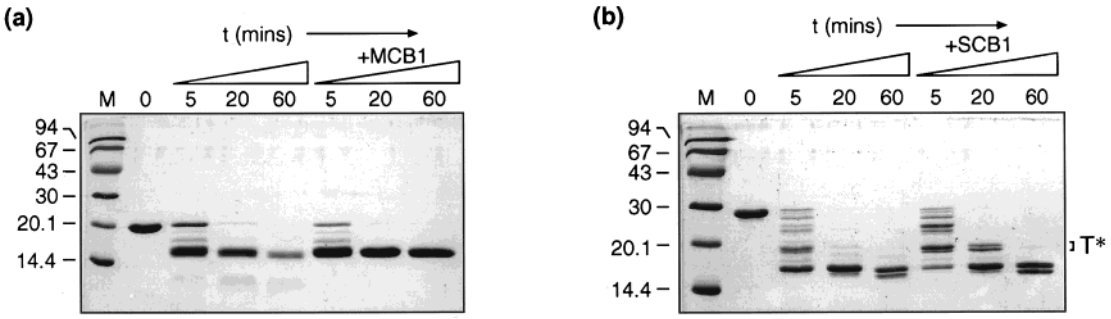

FIGURE 3: Time courses of limited tryptic digestion analyzed by SDS−PAGE. The time of digestion is indicated above each track. The products of digestion of Mbp1(151) and the Mbp1(151)−MCB1 complex [1:250 (w/w) trypsin:protein] are shown in panel a. The products of digestion Swi4(202) and the Swi4(202)-SCB1 complex [1:500 (w/w) trypsin:protein) are shown in panel b. The intermediate species stabilized in the complex are indicated by T*.

A more detailed analysis of the digestion products of both free and complexed Mbp1(151) using ESI-MS allowed the exact sites of proteolytic cleavage to be mapped. Analysis of the products of digestion of Mbp1(151) revealed that cleavage only occurs within the C-terminal nonconserved region and that all products contain the natural N-terminus. The major species produced by digestion of free protein was found to contain six different polypeptides resulting from cleavages at Lys 116, Lys 122, Arg 125, Lys 126, Lys 127, and Arg 130. In contrast, analysis of the digestion products of the DNA−protein complex revealed only three fragments corresponding to cleavages at Arg 125, Lys 126, and Lys 127. The presence of the DNA duplex therefore confers protection from proteolytic digestion at Lys 116 and Lys 122. An equivalent analysis of the products of digestion of Swi4-(202) also reveals differences between free protein and Swi4-(202)−SCB complex. In this case, unlike Mbp1, digestion of Swi4 also occurs at the N-terminus at Lys 24 together with cleavages within the C-terminal region at Arg 156 and Lys 157. ESI-MS analysis of the T* intermediates from an early time point in a Swi4(202)−SCB1 digestion allowed identification of a protected peptide corresponding to residues Ser 25−Lys 177. Based on the preliminary DNA binding data, the proteolysis results, and sequence alignments, three new constructs were prepared: Mbp1(124), which encompasses all of the protected region, and two Swi4 fragments, Swi4(32−178) and Swi4(32−173). Swi4(32−178) and Swi4-(32−173) behave identically in terms of their DNA-binding activity and have all 30 of the nonconserved N-terminal residues of Swi4 deleted (see Figure 1c). Gel-retardation analysis shows that removal of this region does not affect the DNA-binding activity of any Swi4 fragment that we have examined (data not shown).

In Vitro DNA-Binding Characteristics of N-Terminal Domains from Mbp1 and Swi4. Gel-Retardation Assays: Affinity and Stoichiometry. The DNA-binding specificity and affinity of Mbp1(124) and Swi4(32−173) were investigated by a combination of gel-retardation titration and competition experiments. The former allows the stoichiometry and affinity for the specific interaction with MCB or SCB elements to be determined, whereas competition experiments allow the specificity of the interaction to be investigated. They can be

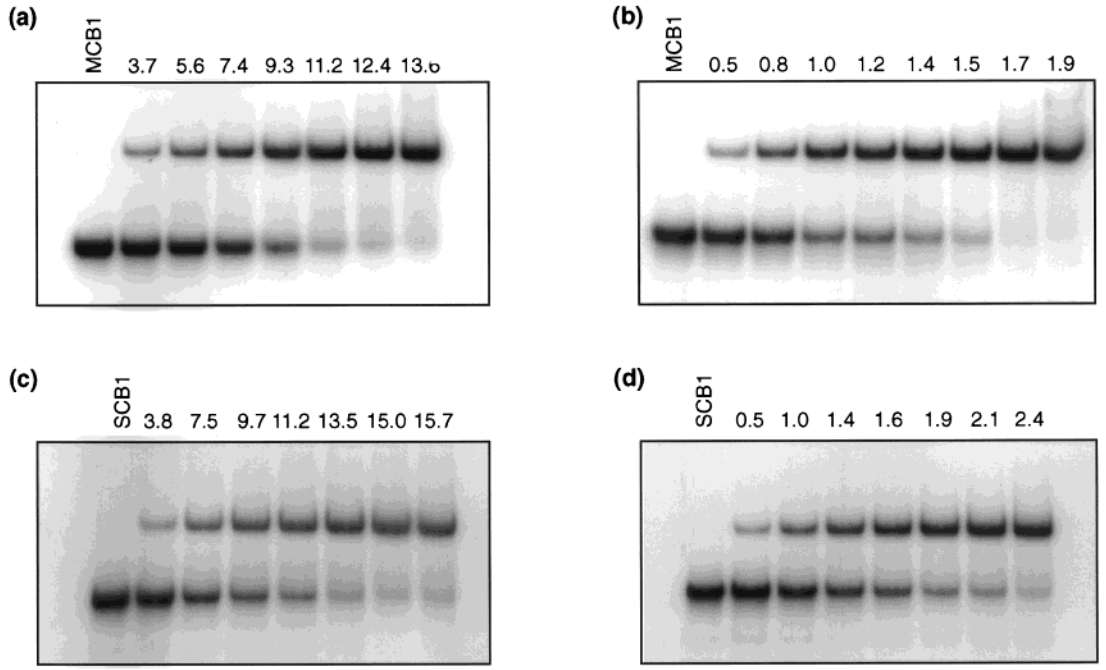

FIGURE 4: Gel-retardation titration assays of proteolytically defined DNA binding domains from Mbp1 and Swi4. Panels a and b show titrations of Mbp1(124) with MCB1 at 11.8 and 1.1 μM. Panels c and d show titrations of Swi4(32−173) with SCB1 at 13.2 and 1.3 μM. The protein concentration (micromolar) is indicated above each track.

used to derive apparent binding constants for both noncognate sites and nonspecific DNA, and therefore define the selectivity of the proteins for DNA sequences (*28*).

Protein/DNA titrations of Mbp1(124) and Swi4(32−173) against MCB and SCB oligonucleotides are shown in Figure 4. These were carried out at both "high" (~10 μM) and "low" (~1 μM) concentrations of binding sites, from which both the stoichiometry and apparent association equilibrium constants, respectively, can be accurately determined. The high binding site concentration titration of MCB1 with Mbp1(124) and that of SCB1 with Swi4(32−173) are shown in Figure 4, panels a and c. In both cases, saturation of binding occurs when the concentrations of protein and duplex are equal, clearly demonstrating that the stoichiometry for both of these interactions is one protein molecule per binding site. Furthermore, a 1:1 stoichiometry was also observed for the interaction of Mbp1(124) with a short 12 bp MCB-containing duplex (MCB12T) in solution binding experiments monitored by ^{1}H NMR and CD spectroscopy (see below). Experiments carried out at lower DNA and protein concentration are shown in Figure 4b,d. From these data, association constants of $(4.0 \pm 1.6) \times 10^6$ M^{-1} and $(1.2 \pm 0.3) \times 10^6$ M^{-1} were calculated for the Mbp1(124)−MCB1 and Swi4(32−173)−SCB1 interactions, respectively (Table 1). Thus, both proteins have similar affinities for their cognate DNA sites.

Gel-Retardation Assays of Site-Directed Mutants. To probe the roles of the protected lysine residues in the C-terminal region of Mbp1, three site-directed mutant proteins were constructed: K116A, K122A, and the double mutant K116A/K122A. In all three molecules, the apparent affinities for the MCB1 oligonucleotide duplex were reduced with respect to the wild-type protein. The smallest effect observed was a ~3-fold reduction in K_a for K122A compared with a more significant ~10-fold reduction for the K116A mutation (Figure 5a). In combination, these two lesions result in a molecule that resembles Mbp1(110) in its DNA-binding activity (compare Figure 5b with Figure 2a), unequivocally demonstrating the functional importance of these basic residues within the tail region of Mbp1.

Table 1: Summary of DNA-Binding Data for Mbp1(124) and Swi4(32−173)

protein	K_A[a] (M^{-1})	K_{comp}[b] (M^{-1})	K_A/K_{comp}[c]	K_{NS}[d] (M^{-1})	K_A/K_{NS}[e]
Mbp1(124)	$(4.0 \pm 1.6) \times 10^6$	7.3×10^5	5.5	1.0×10^4	400
Swi4(32−173)	$(1.2 \pm 0.3) \times 10^6$	2.1×10^5	5.7	8.4×10^3	140

[a] Association constants determined by titration for the specific interaction of Mbp1(124) with MCB binding site and Swi4(32−173) with an SCB binding site. Errors are standard deviation taken from at least three independent experiments. [b] Association constants derived from competition experiments, for Mbp1(124) with an SCB site and Swi4(32−173) with an MCB site. [c] Specificity ratio for site preferences: for Mbp1(124) the ratio of MCB:SCB binding, and for Swi4(32−173) the ratio of SCB:MCB binding. [d] Association constants for Mbp1(124) and Swi4(32−173) with nonspecific DNA, derived from competition experiments. [e] Specificity ratio for specific binding relative to nonspecific DNA: for Mbp1(124) the ratio of MCB:NS-DNA, and for Swi4(32−173) the ratio of SCB:NS-DNA.

Gel-Retardation Competition Assays: *Binding Specificity*. To analyze the specificity of the protein−DNA interactions, two kinds of competition experiments were carried out. First, we estimated the degree of nonspecific binding to sonicated *E. coli* DNA with an average length of ~ 200 bp. Second, we quantified the cross-competition between Mbp1 and Swi4 with their respective cognate sites. Sonicated *E. coli* DNA can be considered to be a series of equivalent but overlapping binding sites one base pair apart (*29*). As the average length of the nonspecific DNA is much greater than a MCB or SCB binding site, the concentration of nonspecific sites is equal to the concentration of base pairs. The competition experiments used to analyze the specificity of Mbp1(124) and Swi4(32−173) are shown in Figure 6, and results are

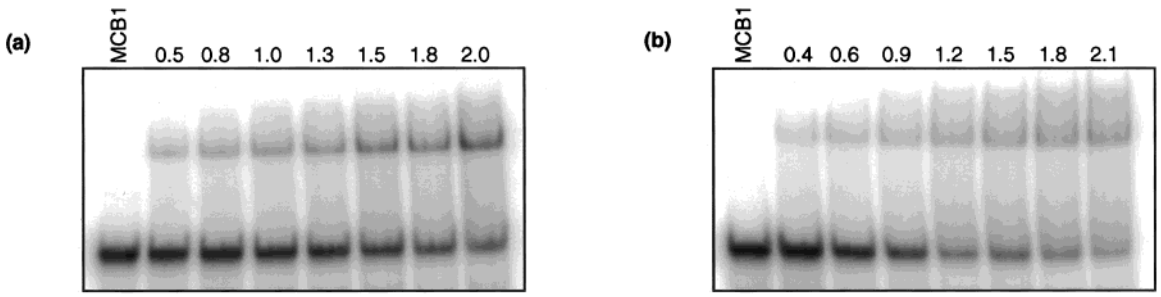

FIGURE 5: Analysis of the DNA-binding properties of Mbp1(124) mutants by gel-retardation titration assay. (a) titration of 1.3 μM MCB1 with K116A; (b) titration of 1.5 μM MCB1 with K116A/K122A. The protein concentration (micromolar) is indicated above each track.

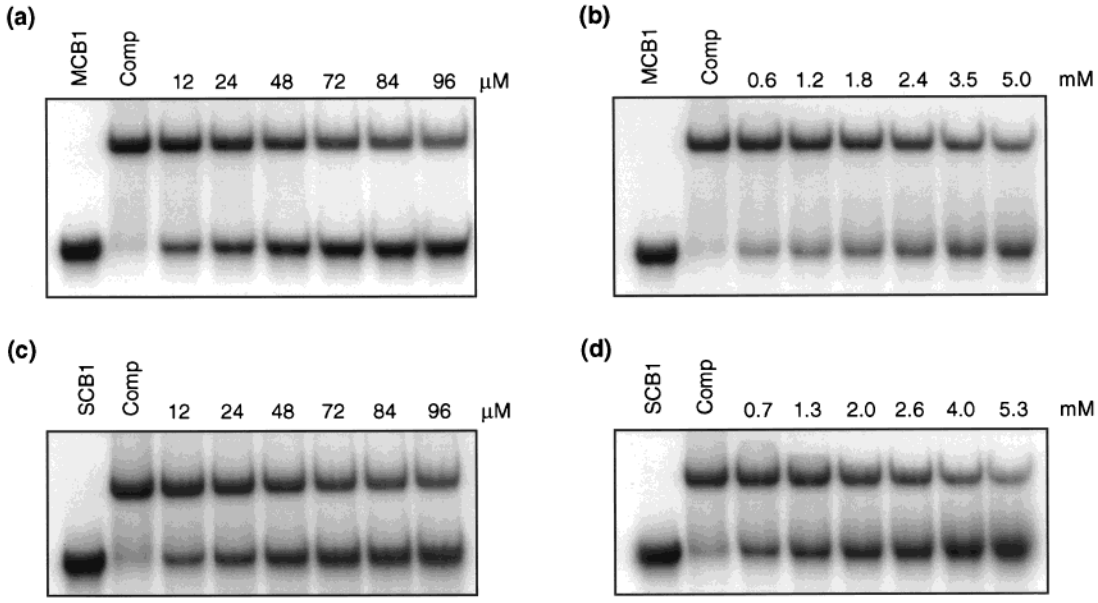

FIGURE 6: Gel-retardation competition experiments with MCB1 (11.6 and 12.0 μM, panels a and b) or SCB1 (12.9 and 13.2 μM, panels c and d). On all gels track 1 is free DNA and track 2 is an equimolar mixture of duplex with either Mbp1(124) in panels a and b or Swi4(32−173) in panels c and d. The concentration of unlabeled competitor DNA added is indicated above each track, which in panel a is SCB1, in panel c is MCB1, and in panels b and d is sonicated *E. coli* DNA.

summarized in Table 1. A striking feature of these data is the effectiveness with which SCB elements compete with MCB elements for Mbp1(124) binding. Similarly, MCB elements compete strongly with the SCB duplex for Swi4-(32−173) binding. In both cases there was only about a 6-fold discrimination between MCB and SCB elements. Nevertheless, both proteins are able to discriminate against nonspecific competitor DNA by a factor of >100.

Circular-Dichroism Titrations. The near-UV absorption band (300−240 nm) of nucleic acids has appreciable CD, which is dominated by helical stacking interactions between bases (*30*). The absorbance and CD of proteins in this region is generally much weaker than DNA. Therefore, near-UV CD spectroscopy allows selective monitoring of the DNA component of a nucleoprotein complex. Often, the CD of short DNA duplexes containing protein recognition sites is perturbed by the addition of a specific DNA binding protein (*23*, *31*, *32*). Spectral changes arising from local alterations in DNA conformation upon protein binding can be used to derive the association constant and stoichiometry for the DNA−protein interaction (*33*, *34*).

The CD spectrum of the short oligonucleotide duplex MCB12T and that of MCB12T in complex with Mbp1(124) are shown in Figure 7a. The free MCB12T duplex DNA spectrum is typical of oligonucleotides in the B-form but changes significantly upon formation of the DNA−protein complex. There are small differences in the spectral intensity of both the positive and negative lobes and a large red shift (~6 nm) of the whole spectrum. We have exploited the large differences in CD between the free and bound forms of MCB12T at 270 nm for titration experiments. A plot of the fraction of bound DNA, derived from the change in CD at 270 nm, against the total protein concentration is shown in Figure 7b. Data were best fit to a stoichiometry of one protein per duplex and an equilibrium binding constant of $(3.7 \pm 0.3) \times 10^6$ M^{-1}. The latter value is in close agreement with that determined by gel-retardation assay for Mbp1(124) and MCB1 (Table 1) and indicates that, notwithstanding the nonequilibrium limitations of gel-retardation assays, absolute binding constants measured in this way are reliable for this system.

NMR Spectroscopy of the Mbp1(124)−MCB Interaction. The changes in the CD spectrum of MCB12T suggest that a significant alteration in DNA structure occurs upon binding to Mbp1(124). Unfortunately, although such changes in nucleic acid CD are common, they are not easily interpretable in terms of the roll, twist, propeller twist, or tilt parameters used to describe DNA structure. Instead, we have used NMR

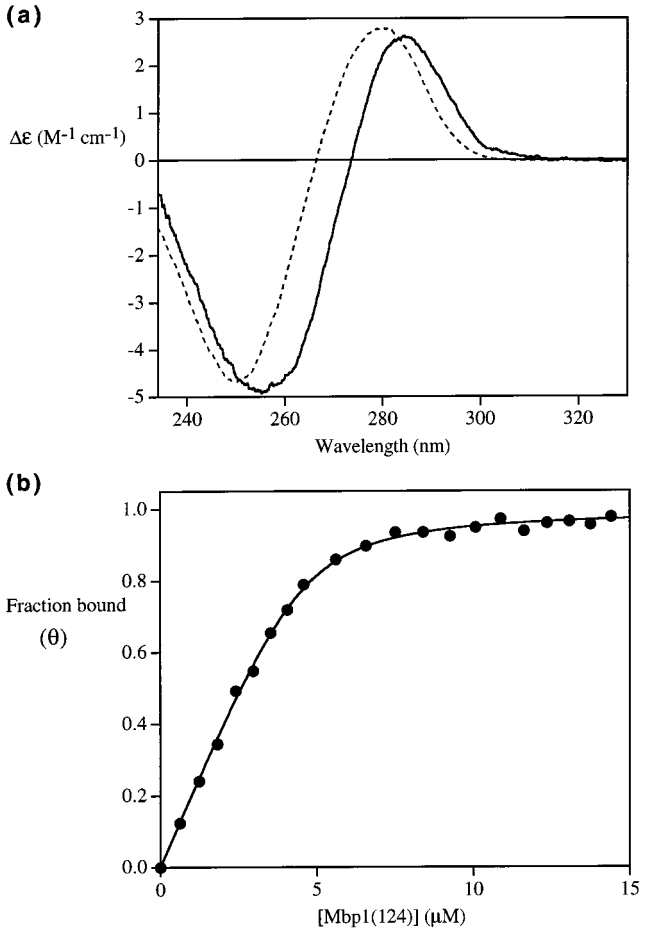

FIGURE 7: (a) Near-UV CD spectra of MCB12T, free (4.68 μM, dashed line) and in complex with Mbp1(124) (solid line). Data are expressed in $\Delta\epsilon$ per nucleotide. (b) Binding curve generated from a titration of 4.68 μM MCB12T with Mbp1(124). Data were corrected for protein and solvent contribution and plotted as θ (fraction of MCB12T sites saturated) versus total Mbp1(124) concentration. The curve is the line of best fit to these data.

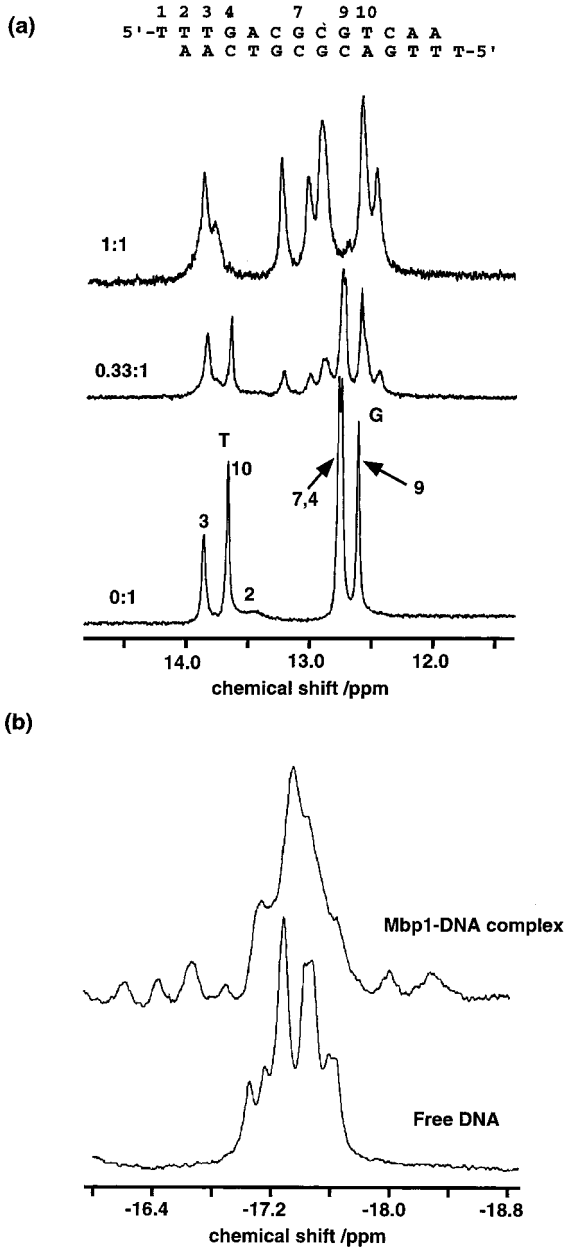

FIGURE 8: (a) Titration of MCB12T with Mbp1(124) monitored by the ^{1}H NMR spectrum of MCB12T, imino region. Spectra are arranged such that the concentration of Mbp1(124) increases from the bottom to the top of the figure. The ratio of protein to DNA is indicated. (b) ^{31}P NMR spectra of MCB12T (lower) and Mbp1(124)−MCB12T complex (upper).

spectroscopy to further investigate structural changes in the DNA.

The proton resonances of free MCB12T have been previously assigned (*24*). In agreement with the CD data, the NMR spectrum is typical of an oligonucleotide with a B-form structure. To examine the effect of protein binding, MCB12T was titrated with increasing concentrations of Mbp1(124) and binding was monitored as a function of the changes in chemical shift of the DNA imino protons (Figure 8a). The self-complementary free DNA shows only six NH resonances (the terminal T2N3 proton is broadened by exchange with solvent). On addition of Mbp1 the imino proton resonances of the free DNA remain sharp and unshifted, and a new set of broader, shifted resonances appear (cf. 0.33:1 molar ratio in Figure 8a). The appearance of two sets of peaks indicates that the binding and dissociation are slow on the chemical shift time scale (<250 Hz). At a ratio of 1:1, the free DNA peaks have essentially disappeared, revealing at least seven different resonances that are substantially broader (>2-fold) than those of the free DNA. This both confirms the 1:1 stoichiometry and indicates that the dyad symmetry of the DNA has been broken by the formation of asymmetric contacts in the 1:1 complex. The movement of the peaks for the imino protons 4−10 but not 3 indicates binding in the G-rich portion of the duplex. This may involve changes in the conformation of the DNA itself since the imino protons are unlikely to make direct contact with protein side chains. Further indication of binding and possible conformational changes in the DNA are shown by ^{31}P NMR spectra (Figure 8b). The free DNA spectrum is typical for duplex DNA, with a shift dispersion of <0.6 ppm. The spectrum of the 1:1 protein−DNA complex exhibits significant line-broadening as a result of the increase in molecular size. In addition, there are four peaks upfield and two peaks downfield of the main group. The appearance of both upfield- and downfield-shifted ^{31}P NMR peaks in DNA−protein and DNA−ligand complexes has been observed in a number of systems (*35*−*37*). It has been suggested that these shifts are associated with changes in

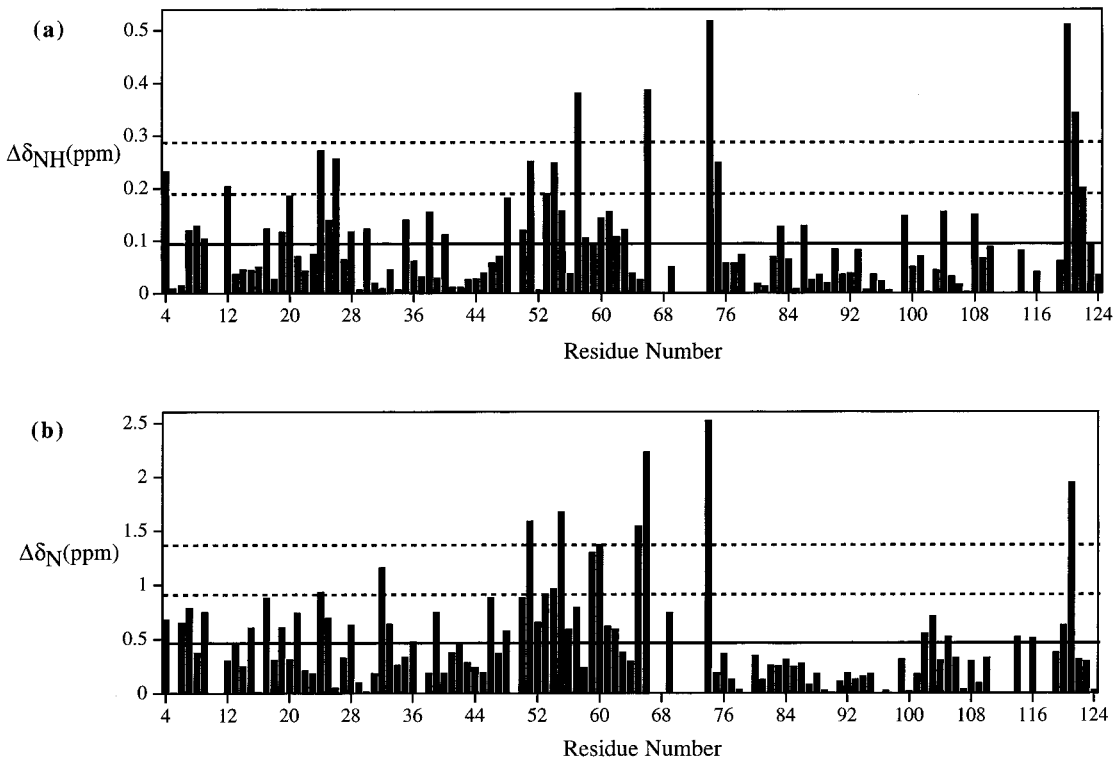

FIGURE 9: Changes in backbone chemical shifts between free and bound Mbp1(124). The magnitudes of the differences in the amide proton (a) and backbone nitrogen (b) are plotted against sequence number. Gaps in the histogram indicate the positions of prolines and other backbone resonances that have not been assigned. The solid line represents the mean chemical shift difference, and the dotted lines are 1 and 2 standard deviations from the mean.

backbone torsion angles such as the B_I to B_{II} conformation transition (*38*) and other conformations (*39*, *40*).

Chemical Shift Mapping of the Protein−DNA Complex. An essentially complete backbone assignment of Mbp1(124) and a Mbp1(124)−MCB12T protein−DNA complex has been obtained from heteronuclear ^{1}H, ^{13}C, and ^{15}N double and triple resonance experiments (*24*). Changes in the observed backbone amide nitrogen and proton chemical shifts of Mbp1(124) upon formation of a complex with MCB12T are plotted in Figure 9; no significant changes in either the Cα or Hα are observed (data not shown). As the Cα and Hα chemical shift is generally more sensitive to alterations in secondary structure (*41*, *42*), this indicates that the differences that arise in the amide nitrogen and proton are likely to be a result of small perturbations in local side chain/main chain conformation rather than large changes in protein secondary structure upon DNA binding.

The analysis of chemical shift changes can be used to map the position of ligand-, protein-, and DNA-binding surfaces on proteins (*43*−*47*). In this case, the overall changes in chemical shifts are not large but are comparable with those seen with other DNA-binding proteins upon complex formation (*46*, *47*). As mentioned previously, we and others have proposed that an $\alpha_2\beta_2$ wHTH motif, which is associated with regions of positive electrostatic potential, is a likely interaction surface for DNA in these proteins (*20*, *21*; Figure 10a,b). Here we show that almost all of the significant chemical shift differences that occur upon DNA binding by Mbp1 fall within two clusters of residues (Figure 9). The first consists of residues 50−74 from αB, β5, and β6. Together these residues form part of the proposed recognition motif. The pattern of the most significant chemical shift differences for residues within the core domain structure can be mapped onto the molecular surface of the molecule (Figure 10c). This defines a ridge along the surface of the protein that corresponds to one face of αB and the loop preceding β5 that is, itself, flanked by regions of positive electrostatic potential (Figure 10a,b). These basic surfaces are associated with conserved lysine and arginine residues that presumably interact with the phosphate backbone. These contacts position the recognition helix such that side chains on the intervening ridge may then penetrate the major groove and form base-specific contacts with the DNA bases. The second region that exhibits large shift changes encompasses residues 120−122 within the C-terminal tail. This region of the protein is disordered in the crystal structures (*21*) and appears to be much more dynamic than the core of the protein in solution (McIntosh et al., unpublished data). The large shift differences in this region of the protein are, again, consistent with its importance for full DNA-binding activity.

DISCUSSION

Full DNA Binding Requires a Nonconserved C-Terminal Region. The gel retardation experiments demonstrate substantial differences in DNA-binding activity between proteins containing only the core domain and those that include the extra C-terminal sequences. The extended domains show a significant enhancement in binding compared with the core domains and are able to form stoichiometric complexes. The notion that sequences C-terminal to the core homology domain are required for full specific DNA binding to MCBs and SCBs is further supported by the results of our proteolysis experiments. These demonstrate that lysine and arginine residues within a ∼25 amino acid region outside

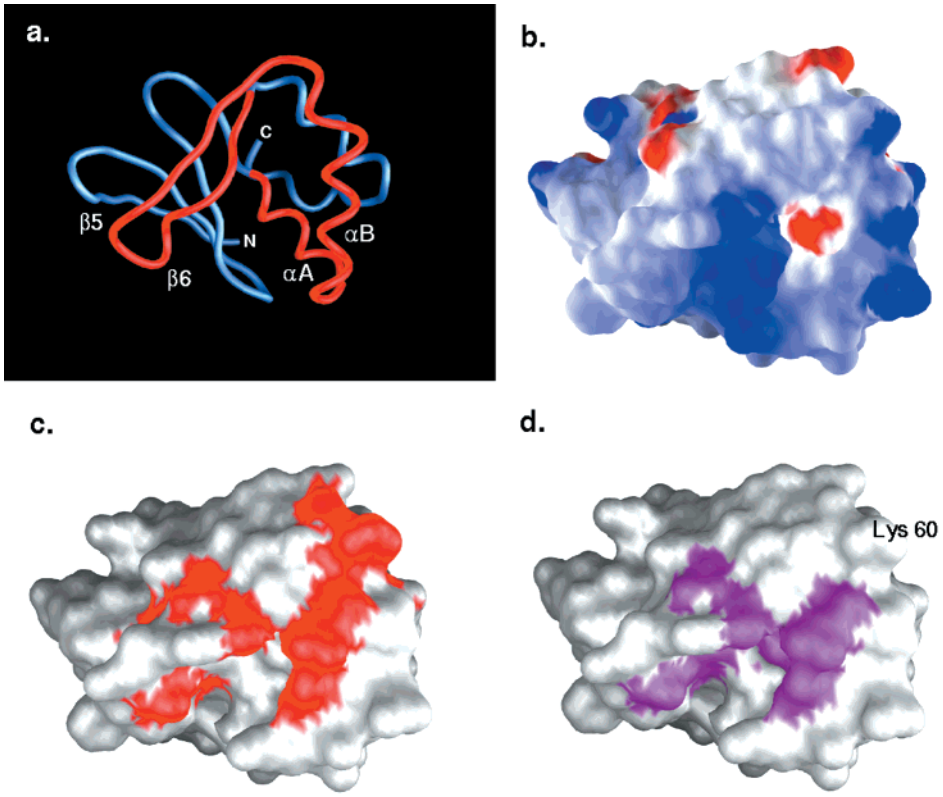

FIGURE 10: (a) Structure of the DNA-binding domain of Mbp1, shown as a worm representation. The putative wHTH motif is highlighted in red. (b) Electrostatic potential surface with positive potential colored blue and negative red with neutral in white, contoured at $\pm 10kT$. The view is the same as in panel a. (c) Chemical shift differences ($\geq 2\sigma$) of Mbp1(124) between the free and DNA-bound molecule mapped onto the molecular surface. (d) Comparison of sequence homology with chemical shift differences. The most significant shift changes in the protein/DNA complex are associated almost exclusively with absolutely conserved residues. These are predominantly associated with the face of the proposed recognition helix B. Lys 60 is an exception and its substitution for aspartate in Swi4 likely removes a phosphate backbone contact.

the core homology domain of both Swi4 and Mbp1 are protected from digestion by trypsin in the presence of their cognate DNA sequences. Mutagenesis of Lys 116 and Lys 120 within the tail of Mbp1 is sufficient to reduce the apparent affinity almost to that observed for the truncated Mbp1(110) protein. Previous studies have shown that an N-terminal 138-residue fragment of Swi4, which includes all of the core sequence, is not sufficient for binding to SCB elements within the CLN2 promoter (*19*). A fragment extending to residue 155 does exhibit DNA binding activity in vitro, but we have now demonstrated that specific, high-affinity DNA binding requires even larger Swi4 fragments still. Specifically, our data now suggest that the minimum Swi4 fragment that exhibits DNA-binding activity comparable to that of Mbp1(124) extends from residue 32 to around173.

Affinity and Specificity of DNA Binding. We have measured the in vitro DNA binding parameters of proteolytically defined domains derived from the N-termini of Swi4 and Mbp1. Mbp1(124) binds to MCB elements with an affinity of around 4.0×10^6 M^{-1}. The interaction of Swi4(32−173) with a single SCB is slightly weaker with a K_a of 1.2×10^6 M^{-1}. Thus, the Mbp1−MCB and the Swi4−SCB interactions occur with similar affinities. Although our experiments have been carried out with isolated N-terminal domains, we are confident that the data presented accurately describe the essential DNA-binding activities of Swi4 and Mbp1 in the context of the SBF and MBF complexes for two reasons. First, N-terminal fragments of Swi4 produce chemical footprints (*19*) that are identical to those observed in vivo for SBF binding to the CLN2 promoter (*48*) and an SCB−LacZ reporter gene (*49*). Second, the extent of the MBF footprint (*3*) is similar to that observed for Swi4 fragments (*19*) and the SBF complex itself (*48*).

It has been previously suggested that N-terminal fragments of the related Res2 protein bind to MCB elements as dimers (*50*). However, our titration experiments unequivocally demonstrate that the N-terminal domains of Swi4 and Mbp1 bind to MCB and SCB sequences with a stoichiometry of one protein molecule per recognition site. Furthermore, the rotational correlation time measured for Mbp1(124) in ^{15}N relaxation experiments recorded at millimolar concentrations (McIntosh et al., unpublished results) are consistent only with the protein being monomeric, both free and bound to DNA. Given the degree of sequence conservation within this family of proteins, it is likely that this will be true for all members. SBF/MBF-regulated promoters may contain multiple copies of SCB/MCB elements and some evidence of cooperative interactions between MBF complexes bound to repeated MCBs in the TMP1 promoter region has been presented (*3*). However, studies of regulatory DNA sequences associated with cell-cycle-regulated genes in *S. cerevisiae* indicate that <30% of those that possess an MCB sequence contain more than one copy (*51*). We have now shown that both Mbp1 and Swi4 are, in fact, able to interact tightly and specifically with single SCB and MCB sequences in vitro.

Cross-competition of SCBs and MCBs has been noted previously (*3*, *19*) but never quantified. Our competition experiments demonstrate that both Mbp1(124) and Swi4-(32−173) are able to bind specifically to their respective MCB and SCB sequences and discriminate by at least 100-fold in favor of their specific sites versus nonspecific DNA. However, discrimination between SCB and MCB elements by either protein is rather weak. In fact, neither protein exhibits greater than a 5−6-fold preference for its presumed cognate site. It has been shown previously that mutations of the 5′-(CGCG)-3′ core tetranucleotide sequence within the MCB consensus are the most deleterious for Mbp1-directed regulation of the TMP1 promoter in vivo (*8*). Consistent with these data, our NMR titrations show that significant perturbations of DNA structure occur within the central 5′-(CGCG)-3′ region of the MCB element upon protein binding. Thus, the major, and perhaps the only, determinant of binding specificity is a $C^{A}/_{G}CG$ element common to both MCB and SCB sequences. It should be noted, however, that significant effects on SBF/SCB interactions have been reported following mutation of other consensus bases outside the $C^{A}/_{G}CG$ core (*52*). The similarity in DNA-binding site sequence is mirrored in the similarities in amino acid sequences of Mbp1 and Swi4. Mapping of residues that are identical in all members of this family shows that conserved sequences either make up the hydrophobic core of the six-stranded β-barrel or cluster on the $\alpha_2\beta_2$ wHTH region (*21*). Of the residues associated with the presumed DNA-binding motif, only a subset show significant chemical shift differences in the DNA complex, and all of these are conserved with the exception of Lys 60 (Figure 10c,d). This residue is located in a region of rather variable sequence between αB and β5 of wing 1. In Mbp1, Lys 60 contributes to the overall positive electrostatic potential of the domain. However, an aspartic acid occupies the equivalent position in Swi4, suggesting that this residue plays only a minor role in DNA binding by Mbp1 and may contribute to the ∼3-fold higher affinity of Mbp1 compared to Swi4.

Overall, our observations are entirely consistent with the modest discrimination between SCB and MCB elements exhibited by either Swi4 or Mbp1 in vivo. Studies of regulation of CLN1 gene expression have indicated that transcriptional activation is brought about by SBF complexes binding not to SCB elements but to promoter-distal MCB-like sequences (*53*, *54*). Therefore, the range of promoter specificities observed for SBF and MBF in vivo is likely to be a result of interactions with other accessory proteins, variations in chromatin structure, and/or other regulatory effects. For example, interactions between Clb2/Cdc28 and SBF appear to disrupt binding to the CLN2 promoter in G2 (*12*, *48*). Furthermore, several suppressors of mutant Swi6 alleles appear to be transcription factors or architectural DNA-binding proteins (*55*). Finally, many of the remainder of the SWI family of proteins, originally discovered as mutations defective in HO expression (*7*), are now known to be subunits of the SWI/SNF chromatin remodeling complex (*56*).

A Model of DNA Binding. There are numerous examples of DNA-binding proteins that contain extensions to a core domain that are essential for full biological activity. Sequence variations between basic C-terminal regions of otherwise closely related proteins of the GATA family have been shown to result in structurally distinct modes of protein−DNA interaction with concomitant changes in binding activity (*57*). Similarly, the wHTH protein HNF3γ possesses a basic C-terminal tail, wing 2, that stabilizes the DNA complex through phosphate backbone and nonspecific, minor-groove interactions (*22*). The Swi4/Mbp1 family of wHTH proteins all possess a conserved core domain containing an $\alpha_2\beta_2$ motif that is structurally similar to the wing 1 and HTH elements observed in HNF3γ (*20*, *21*). It has been suggested that the wing 2 region of HNF3γ-related molecules has been lost in Mbp1 and replaced by αC and D (*20*). In contrast, the data presented here unequivocally demonstrate a role for residues within the Mbp1/Swi4 tail regions and reveal important, and previously unsuspected, functional similarities between the wing 2 regions of these and other wHTH molecules. However, several important and unusual features are also apparent. First, in other wHTH molecules that use N- or C-terminal extensions in their DNA interactions, these regions tend to be conserved within a family. In marked contrast, the sequences of the tail regions of the Mbp1/Swi4 family are substantially different (Figure 1c). Second, ^{15}N relaxation and NOE data indicate that the Mbp1/Swi4/Res1/Res2 wing 2 regions may play a structural role in these molecules through interactions of tail residues with the core of the protein (McIntosh et al., unpublished data). The NMR chemical shift data presented here reveal changes upon DNA binding that occur both in and around the recognition helix and within the C-terminal region. Thus, the nonconserved tail appears to be responsible for enhancing the DNA-binding activity >50-fold through a combination of intramolecular protein−protein and intermolecular protein−DNA interactions.

ACKNOWLEDGMENT

NMR spectra were recorded at the MRC Biomedical NMR Centre, Mill Hill. We thank Dr. Steve Gamblin for critical reading of the manuscript and the NIMR graphics department for assistance with figure preparation.

REFERENCES

1. Zawel, L., and Reinberg, D. (1995) *Annu. Rev. Biochem. 64*, 533−61.
2. Ptashne, M., and Gann, A. (1997) *Nature 386*, 569−77.
3. Dirick, L., Moll, T., Auer, H., and Nasmyth, K. (1992) *Nature 357*, 508−13.
4. Andrews, B. J., and Herskowitz, I. (1989) *Cell 57*, 21−9.
5. Andrews, B. J., and Moore, L. A. (1992) *Proc. Natl. Acad. Sci. U.S.A. 89*, 11852−6.
6. Koch, C., Moll, T., Neuberg, M., Ahorn, H., and Nasmyth, K. (1993) *Science 261*, 1551−7.
7. Breeden, L., and Nasmyth, K. (1987) *Cell 48*, 389−97.
8. McIntosh, E. M., Atkinson, T., Storms, R. K., and Smith, M. (1991) *Mol. Cell. Biol. 11*, 329−37.
9. Zhu, Y., Takeda, T., Nasmyth, K., and Jones, N. (1994) *Genes Dev. 8*, 885−98.
10. Sedgwick, S. G., Taylor, I. A., Adam, A. C., Spanos, A., Howell, S., Morgan, B. A., Treiber, M. K., Kanuga, N., Banks, G. R., Foord, R., and Smerdon, S. J. (1998) *J. Mol. Biol. 281*, 763−75.
11. Sidorova, J., and Breeden, L. (1993) *Mol. Cell. Biol. 13*, 1069−77.
12. Siegmund, R. F., and Nasmyth, K. A. (1996) *Mol. Cell. Biol. 16*, 2647−55.
13. Breeden, L., and Nasmyth, K. (1987) *Nature 329*, 651−4.

14. Breeden, L. L. (1995) Vol. 28, pp 95−127, Springer-Verlag, Berlin.
15. Foord, R., Taylor, I. A., Sedgwick, S. G., and Smerdon, S. J. (1999) *Nat. Struct. Biol. 6*, 157−65.
16. Nakashima, N., Tanaka, K., Sturm, S., and Okayama, H. (1995) *EMBO J. 14*, 4794−802.
17. Sturm, S., and Okayama, H. (1996) *Mol. Biol. Cell. 7*, 1967−76.
18. Ho, Y., Costanzo, M., Moore, L., Kobayashi, R., and Andrews, B. J. (1999) *Mol. Cell. Biol. 19*, 5267−78.
19. Primig, M., Sockanathan, S., Auer, H., and Nasmyth, K. (1992) *Nature 358*, 593−7.
20. Xu, R. M., Koch, C., Liu, Y., Horton, J. R., Knapp, D., Nasmyth, K., and Cheng, X. (1997) *Structure 5*, 349−58.
21. Taylor, I. A., Treiber, M. K., Olivi, L., and Smerdon, S. J. (1997) *J. Mol. Biol. 272*, 1−8.
22. Clark, K. L., Halay, E. D., Lai, E., and Burley, S. K. (1993) *Nature 364*, 412−20.
23. Taylor, I. A., Davis, K. G., Watts, D., and Kneale, G. G. (1994) *EMBO J. 13*, 5772−8.
24. McIntosh, P. B., Taylor, I. A., Smerdon, S. J., Frenkiel, T. A., and Lane, A. N. (1999) *J. Biomol. NMR 13*, 397−8.
25. Kelly, R. C., Jensen, D. E., and von Hippel, P. H. (1976) *J. Biol. Chem. 251*, 7240−50.
26. Plyte, S. E., and Kneale, G. G. (1993) *Biochemistry 32*, 3623−8.
27. Webb, M., Taylor, I. A., Firman, K., and Kneale, G. G. (1995) *J. Mol. Biol. 250*, 181−90.
28. Taylor, I. A., Watts, D., and Kneale, G. G. (1993) *Nucleic Acids Res. 21*, 4929−35.
29. McGhee, J. D., and Hippel, P. H. v. (1974) *J. Mol. Biol. 86*, 469−89.
30. Johnson, B. B., Dahl, K. S., Tinoco, I., Jr., Ivanov, V. I., and Zhurkin, V. B. (1981) *Biochemistry 20*, 73−8.
31. Fried, M. G., Wu, H. M., and Crothers, D. M. (1983) *Nucleic Acids Res. 11*, 2479−94.
32. Matthews, J. R., Nicholson, J., Jaffray, E., Kelly, S. M., Price, N. C., and Hay, R. T. (1995) *Nucleic Acids Res. 23*, 3393−402.
33. Culard, F., and Maurizot, J. C. (1981) *Nucleic Acids Res. 9*, 5175−84.
34. Carpenter, M. L., and Kneale, G. G. (1991) *J. Mol. Biol. 217*, 681−9.
35. Beckmann, P., Martin, S. R., and Lane, A. N. (1993) *Eur. Biophys. J. 21*, 417−24.
36. Haqq, C. M., King, C. Y., Ukiyama, E., Falsafi, S., Haqq, T. N., Donahoe, P. K., and Weiss, M. A. (1994) *Science 266*, 1494−500.
37. Searle, M. S., and Lane, A. N. (1992) *FEBS Lett. 297*, 292−6.
38. Gorenstein, D. G. (1992) *Methods Enzymol. 211*, 254−86.
39. Chou, S. H., Cheng, J. W., and Reid, B. R. (1992) *J. Mol. Biol. 228*, 138−55.
40. Lane, A. N., Martin, S. R., Ebel, S., and Brown, T. (1992) *Biochemistry 31*, 12087−95.
41. Wishart, D. S., Sykes, B. D., and Richards, F. M. (1992) *Biochemistry 31*, 1647−51.
42. Wishart, D. S., and Sykes, B. D. (1994) *J. Biomol. NMR 4*, 171−80.
43. Farmer, B. T. (1996) *Nat. Struct. Biol. 3*, 995−997.
44. Williamson, R. A., Carr, M. D., Frenkiel, T. A., Feeney, J., and Freedman, R. B. (1997) *Biochemistry 36*, 13882−9.
45. Shekhtman, A., McNaughton, L., Cunningham, R. P., and Baxter, S. M. (1999) *Struct. Fold. Des. 7*, 919−930.
46. Shindo, H., Ohnuki, A., Ginba, H., Katoh, E., Ueguchi, C., Mizuno, T., and Yamazaki, T. (1999) *FEBS Lett. 455*, 63−9.
47. McIntosh, P. B., Frenkiel, T. A., Wollborn, U., McCormick, J. E., Klempnauer, K. H., Feeney, J., and Carr, M. D. (1998) *Biochemistry 37*, 9619−29.
48. Koch, C., Schleiffer, A., Ammerer, G., and Nasmyth, K. (1996) *Genes Dev. 10*, 129−41.
49. Harrington, L. A., and Andrews, B. J. (1996) *Nucleic Acids Res. 24*, 558−65.
50. Zhu, Y., Takeda, T., Whitehall, S., Peat, N., and Jones, N. (1997) *EMBO J. 16*, 1023−34.
51. Wolfsberg, T. G., Gabrielian, A. E., Campbell, M. J., Cho, R. J., Spouge, J. L., and Landsman, D. (1999) *Genome Res. 9*, 775−92.
52. Andrews, B. J., and Moore, L. (1992) *Biochem. Cell. Biol. 70*, 1073−80.
53. Partridge, J. F., Mikesell, G. E., and Breeden, L. L. (1997) *J. Biol. Chem. 272*, 9071−7.
54. Flick, K., Chapman-Shimshoni, D., Stuart, D., Guaderrama, M., and Wittenberg, C. (1998) *Mol. Cell. Biol. 18*, 2492−501.
55. Sidorova, J., and Breeden, L. (1999) *Genetics 151*, 45−55.
56. Peterson, C. L., and Tamkun, J. W. (1995) *Trends Biochem. Sci. 20*, 143−6.
57. Starich, M. R., Wikstrom, M., Arst, H. N., Jr., Clore, G. M., and Gronenborn, A. M. (1998) *J. Mol. Biol. 277*, 605−20.

BI992212I